Bioelectrochemistry 96 (2014) 1–6

Contents lists available at ScienceDirect

Bioelectrochemistry

journal homepage: www.elsevier.com/locate/bioelechem

Electrochemical uranyl cation biosensor with DNA oligonucleotides as receptor layer

Marta Jarczewska, Robert Ziółkowski, Łukasz Górski *, Elżbieta Malinowska

Institute of Biotechnology, Department of Microbioanalytics, Faculty of Chemistry, Warsaw University of Technology, Noakowskiego 3, 00-664 Warsaw, Poland

ARTICLE INFO

Article history:
Received 20 June 2013
Received in revised form 20 November 2013
Accepted 20 November 2013
Available online 1 December 2013

Keywords:
DNA biosensor
Electrochemical biosensor
Uranyl cation
Metals determination
Mixed monolayer

ABSTRACT

The present study aims at the further development of the uranyl oligonucleotide-based voltammetric biosensor, which takes advantage of strong interaction between UO_2^{2+} and phosphate DNA backbone. Herein we report the optimization of working parameters of previously elaborated electrochemical DNA biosensor. It is shown that the sensor sensitivity is highly dependent on the oligonucleotide probe length and the incubation time of sensor in a sample solution. Consequently, the highest sensitivity was obtained for 10-nucleotide sequence and 60 min incubation time. The lower detection limit towards uranyl cation for developed biosensor was 30 nM. The influence of mixed monolayers and the possibility of developing a non-calibration device were also investigated. The selectivity of the proposed biosensor was significantly improved via elimination of adenine nucleobases from the DNA probe. Moreover, the regeneration procedure was elaborated and tested to prolong the use of the same biosensor for 4 subsequent determinations of UO_2^{2+}.

1. Introduction

Surface functionalization with self-assembled monolayers (SAMs) is one of the most intensively studied research area in the recent years. It allows for inexpensive and versatile surface coatings for applications including: control of wetting [1,2] and adhesion [3,4], chemical resistance [5,6], nucleation and growth of crystals on surfaces [7,8], biocompatibility [9,10], sensitization for photon harvesting [11], charge transfer [12,13] or tribology [14,15]. SAMs are also crucial in the development of many modern biosensors. The selectivity of these devices is ensured by various types of biomolecules, applied as receptor layers. Biosensor is a solid-state device which is simply placed in the sample of interest, with no washing, rinsing or additional steps required, and provides useful signal that is proportional to a certain analyte concentration [16,17]. The self-assembled monolayers offer the possibility of tuning the properties of a biosensor receptor layer by adjusting the position and density of biomolecules, both vertically and laterally [15,18,19].

Self-assembled monolayers are very often applied for the preparation of electrochemical nucleic acid (NA) biosensors, which utilize dsDNAs, ssDNAs, RNAs, aptamers and DNAzymes as the recognition elements immobilized on the electrodes' surfaces [20]. NA biosensors are dedicated to detect complementary DNA strands, organic or inorganic compounds, bacteria or viruses [16,21,22]. As nucleic acids are electroactive, it is possible to detect the DNA hybridization or damage via analysis of nucleobases' oxidation signals e.g. guanine [20,23]. The label-free approach can also be employed in the determination of redox active analytes such as dopamine [24] or metal cations [25], however it is less sensitive in comparison to the label-based techniques [23]. On the contrary, with the utilization of redox labels lower detection limits can be reached [26]. The redox markers can be either covalently attached to the probe/target sequence or serve as the 'external' labels, which interact with DNA receptor layer via intercalation, groove binding or electrostatic attraction/repulsion. The most commonly used electroactive indicators are: ethidium bromide, $Ru(NH_3)_6^{3+}$, bipyridine complexes of cobalt and anthraquinone [26]. To further improve the analytical parameters of nucleic acid biosensors the electrode's modifications with the introduction of nanoparticles [23], graphene oxide [27] and carbon nanotubes [28] were proposed. Very recently, a number of publications describing direct or indirect electrochemical detection of heavy metal ions with DNA sensors have been published, including devices for the determination of cadmium [29], mercury [30–34], lead [35,36], silver [37–39] and uranyl [40] cations in solution. Such electrochemical biosensors seem to be attractive analytical tools due to low cost, simplicity of their construction, low analyte consumption and small dimensions.

Electrochemical sensors for uranyl cation determination are typically electrodes modified with phosphate-containing compounds, such as: 2-mercatpoethanol/$POCl_3$, cysteamine/2-aminoethyl dihydrogen phosphate or (t-butylphenyl)-N,N-di-(isobutyl) carbamoylmethylphosphineoxide [41–43]. In our previous paper, we described an electrochemical UO_2^{2+} sensor based on 20-base oligonucleotide receptor monolayer [40]. Methylene blue (MB) – a cationic compound with strong affinity to ssDNA and dsDNA, was used as a redox indicator [44]. MB interacts with double-stranded DNA mainly via intercalation, groove binding

* Corresponding author. Tel.: +48 222 347573; fax: +48 226 282741.
E-mail address: lukegor@ch.pw.edu.pl (Ł Górski).

1567-5394/$ – see front matter
http://dx.doi.org/10.1016/j.bioelechem.2013.11.003

and electrostatic attraction and in case of single stranded DNA the electrostatic interaction and affinity towards guanine are the main modes of interaction [26,45].

The operation of this sensor relies on strong interaction between uranyl cation and phosphate residues of the DNA backbone. Due to electrostatic repulsion, MB is forced out of the receptor layer by UO_2^{2+} cation, causing the diminishing of the redox current. Thus, the decrease in methylene blue current is proportional to the concentration of uranyl cation in the sample solution. Despite its relative simplicity, proposed biosensor exhibited some beneficial parameters, especially the lower detection limit of 30 nM for UO_2^{2+}, which is below its maximum contaminant level in drinking water defined by the U.S. EPA (130 nM) [46]. It was also reported that other parameters require further improvement.

In this work, optimization of the receptor layer for DNA-based UO_2^{2+} biosensor is described. The oligonucleotide probe length and sequence varied and the electrode surface area was also altered. Moreover, the effect of additional electrode surface passivation on sensor performance was shown. The procedure of receptor layer regeneration was also developed in order to perform multiple determinations with the use of a single sensor.

2. Materials and methods

2.1. Apparatus

Voltammetric measurements were performed with a CHI 660A and CHI 1040A electrochemical workstations (CH Instruments, USA). The experiments were carried out with a conventional three-electrode system consisting of a gold disk electrode (CH Instruments, USA), a gold wire auxiliary electrode and an Ag/AgCl/1.0 M KCl reference electrode. All potentials are reported versus Ag/AgCl reference at room temperature. The cyclic voltammetry was conducted at a sweep rate of 100 mV/s while the square wave voltammetry was performed at a pulse amplitude of 25 mV, increment of 4 mV and a frequency of 15 Hz.

2.2. Reagents

Tris–HCl, methylene blue (MB), $(CH_3COO)_2UO_2$, $Pb(NO_3)_2$, KH_2PO_4, NaOH, NaCl, EDTA, 6-mercapto-1-hexanol (MCH) were purchased from Aldrich Chemicals. H_2SO_4, H_2O_2, CH_3COOH, $NH_{3(aq)}$ were acquired from POCh, Poland. All reagents were used without further purification. All solutions were prepared with Milli-Q water. Milli-Q water and all aqueous buffer solutions were sterilized using an autoclave. Deoxyoligonucleotides were purchased from Genomed Sp. z o.o., Poland.

The base sequences of the thiolated DNA probes were as follows:

- 5′-SH-$(CH_2)_6$-CGACTGTGAATTCGTAGCAG-3′ (20-base probe sequence);
- 5′-SH-$(CH_2)_6$-CGACTGTGAATTCGT-3′ (15-base probe sequence);
- 5′-SH-$(CH_2)_6$-CGACTGTGAA-3′ (10-base probe sequence);
- 5′-SH-$(CH_2)_6$-CGACTG-3′ (5-base probe sequence);
- 5′-SH-$(CH_2)_6$- TTTGGGTAGGGCGGGTTGGG-3′ (20-base probe sequence);
- 5′-SH-$(CH_2)_6$-CGGCTGTGCGTTCGTCGCGG-3′ (20-base probe sequence).

The oligonucleotide stock solutions were prepared with 10 mM Tris–HCl buffer solution, (pH 7.5) and stored at −20 °C before use.

2.3. Solutions

The following solutions were prepared: piranha solution (H_2O_2/H_2SO_4; 1:3), immobilization buffer solution (1 M KH_2PO_4, pH 4.5), Tris–HCl buffer solution (50 mM), mercaptohexanol solution (4 μM in immobilization buffer), ammonium acetate solution (50 mM CH_3COONH_4) containing 50 mM NaCl and 1 mM EDTA, $Pb(NO_3)_2$ solution (0.4 μM) in 50 mM Tris–HCl solution containing 50 μM methylene blue (pH 3.0). The electrochemical measurements were carried out in 50 mM Tris–HCl containing 50 μM methylene blue and/or uranyl acetate (pH 3.0).

2.4. Methods

Before the electrochemical experiments, the gold disk electrodes were polished with alumina powder of grain sizes from 1 to 0.05 μm (CH Instruments, USA). Then electrodes were washed with water and sonicated for 5 min in demineralized water at 40 º C. Next, the piranha solution was dropped on the working gold disk electrode and incubated for 1 min. After removing the solution, the electrode was again washed with demineralized water. The last step of electrode cleaning was its voltammetric cycling in 50 mM Tris–HCl solution (pH 3.0), until the CV characteristic for a clean gold was obtained.

The DNA recognition monolayer was prepared as described in [47]. Briefly, after the electrode cleaning, the 4 μM solution of thiolated ssDNA in 1 M KH_2PO_4 (pH 4.5) was dropped on the gold working disk electrode. The ssDNA immobilization was performed for 120 min. Next, the solution was removed and the electrode was washed with 1 M KH_2PO_4 (pH 4.5). Subsequently (if needed) electrode was incubated in the 4 μM solution of MCH for 60 min. Finally, the solution was removed, the electrode was washed with immobilization buffer solution and the electrochemical measurements were conducted.

3. Results and discussion

The investigations described below are a direct continuation of experiments described earlier in [40], showing the possibility of uranyl ion detection with ssDNA-modified gold electrodes. In full analogy to previous report, methylene blue (MB) was employed as a redox label in this work. After the incubation of ssDNA-modified gold electrode in MB solution, an electrostatic interaction between cationic redox label and negatively charged DNA receptor layer is observed. As a result, a MB current signal of certain value is registered and it depends on the the incubation time in MB solution as well as on the ssDNA probe length. Then, after the incubation of working electrode in the uranyl acetate solution, the complexation of UO_2^{2+} ions by DNA phosphate moieties occurs. This leads to the competition between methylene blue and uranyl cation and eventually the MB is withdrawn from the recognition layer. As a result, a significant drop in the methylene blue current signal is observed, allowing quantitative uranyl ion determination (Scheme 1).

The sensor response, Δ, is defined as a change of MB peak current, registered in SWV measurements, using the following Eq. (1):

$$\Delta = (I_0\text{-}I)/I_0 \quad (1)$$

where:

I_0 The MB current before the subjection of the sensor to sample solution.

I The MB current after the subjection of the sensor to sample solution.

The previous article [40] reported the analytical parameters of proposed sensor, such as lower detection limit, linear range and selectivity. The results of these investigations were quite promising, thus further experiments were conducted in order to optimize the analytical response of proposed biosensor. These investigations include the influence of oligonucleotide probe sequence and length, additional electrode surface passivation, electrode surface area, and receptor layer regeneration on the biosensor response.

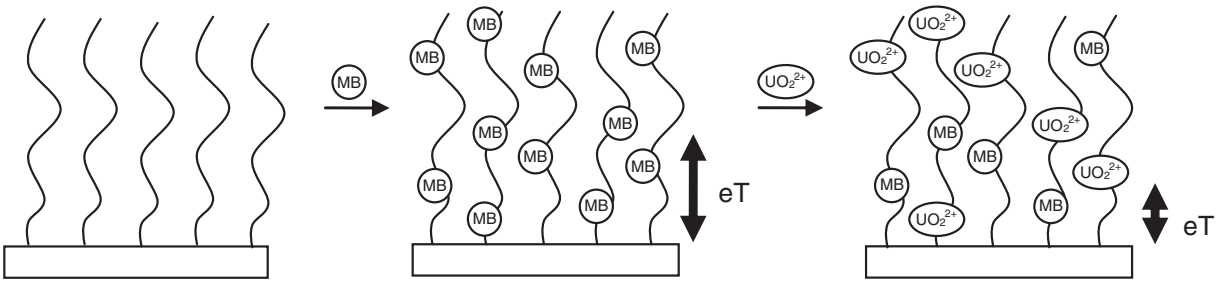

Scheme 1. Schematic representation of biosensor working mechanism. The methylene blue current value was measured before and after subjection of the sensor to the uranyl acetate solution.

3.1. Selectivity optimization

As it was already reported in [40], the strongest interference among examined cations was observed for Pb^{2+} cation. According to literature reports, Pb^{2+} preferably interacts with adenine residues of DNA [25]. Therefore, efforts to diminish interferences from Pb^{2+} on UO_2^{2+} determination by reducing the number of adenine residues in ssDNA probe were undertaken. The following sequences, which differ in a number of adenine residues, were employed in these experiments: 5′-SH-$(CH_2)_6$-CG**A**CTGTG**AA**TTCGT**A**GC**A**G-3′ (probe A, results published in [33]), 5′-SH-$(CH_2)_6$-TTTGGGT**A**GGGCGGGTTGGG-3′ (probe B), 5′-SH-$(CH_2)_6$-CGGCTGTGCGTTCGTCGCGG-3′ (probe C). The measurements were performed with a 5 min incubation time (the concentration of Pb^{2+} and UO_2^{2+} cations was 0.4 μM) and each measurement was repeated four times (Table 1).

As shown in Table 1, a significant difference in selectivity towards lead cation for different ssDNA sequences is observed. Electrode modified with oligonucleotide A, which contains 5 adenine bases shows relatively high Δ value, while Δ for electrode with DNA probe C, containing no adenine, is much smaller. It should be noted that the sensor response towards UO_2^{2+} cation is largely independent of ssDNA probe sequence, as it can be observed in Table 1. This can be explained by the working mechanism of these sensors, based on the interaction of UO_2^{2+} with phosphate backbone of the ssDNA probe. Regardless of the qualitative composition of the nitrogenous bases, the number of binding phosphate residues remains unchanged. It is therefore evident that successive reduction of number of adenine bases in ssDNA probe sequence leads to the lessening of lead interference in UO_2^{2+} determination for proposed sensors.

3.2. Oligonucleotide probe length

The length of oligonucleotide probe is of special importance for DNA sensors, as it determines the number of binding sites in the receptor layer. On the one hand, the number of binding sites can affect the method sensitivity. On the other hand, longer oligonucleotides (over 11 bases) are prone to bending, which can influence monolayer properties [48].

Table 1
Comparison of the selectivity towards Pb^{2+} and UO_2^{2+} ions for DNA biosensors modified with 20-base DNA probes differing in the number of adenine bases.

Oligonucleotide probe	$(I_0-I)/I_0$[d] UO_2^{2+} ion	$(I_0-I)/I_0$ Pb^{2+} ion
Probe A[a]	0.212 ± 0.012	0.120 ± 0.008
Probe B[b]	0.230 ± 0.028	0.085 ± 0.014
Probe C[c]	0.215 ± 0.015	0.054 ±0.008

[a] Probe sequence: 5′-SH-$(CH_2)_6$-CGACTGTGAATTCGTAGCAG-3′
[b] Probe sequence: 5′-SH-$(CH_2)_6$-TTTGGGTAGGGCGGGTTGGG-3′
[c] Probe sequence: 5′-SH-$(CH_2)_6$-CGGCTGTGCGTTCGTCGCGG-3′
[d] I_0 —the MB current before the subjection of the sensor to sample solution; I —the MB current after the subjection of the sensor to sample solution.

A set of experiments was conducted with the use of oligonucleotides of sequences similar to the probe (20 bases) used in the preliminary investigations. Oligonucleotides shortened by 5, 10 or 15 bases were used and various periods of sensor incubation in uranyl ion solution were applied and the obtained calibration curves were compared (Fig. 1). For each sequence, it is noticeable that the slope of the calibration curve increases significantly with the elongation of incubation time. It is also evident that the length of ssDNA probe has a great effect on the sensor sensitivity. For all incubation times longer than 5 min, highest sensitivity was observed for 10-nucleotide sequence. It can be postulated that shorter, 5-nucleotide sequence offers relatively few binding sites (phosphate groups) for UO_2^{2+} ion, resulting in lower slopes of the calibration curves. Lower sensitivity, observed for sensors modified with 15- and 20-nucleotide probes, can be attributed to the oligonucleotide folding.

Taking into account the importance of the short analysis time in standard analytical practice, a 5 min incubation time was chosen to show calibration curves towards uranyl ion for sensors modified with oligonucleotides of different length (Fig. 2). As it can be observed, the sensitivity increases with the elongation of the DNA probe, although observed differences are not very large. This can be rationalized by the fact that during 5 min of sensor incubation in sample solution, only small part of the binding sites of the receptor layer is being occupied by the UO_2^{2+} cation.

It can be concluded that the sensitivity of oligonucleotide-based biosensor can be widely tuned by adjusting probe length and sample incubation time.

3.3. Electrode passivation

The mercaptohexanol electrode surface passivation is widely used in DNA sensors to eliminate the non-specific interactions between gold surface and receptor monolayer or sample constituents. It is especially

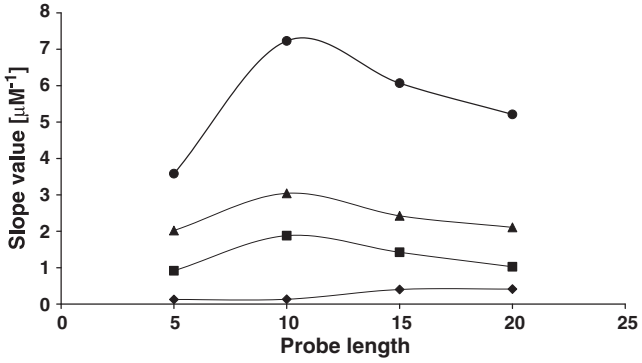

Fig. 1. Comparison of slope values of UO_2^{2+} calibration curves obtained for ssDNA-modified electrode for 5, 10, 15 and 20-base probe sequence: (♦) 5, (■) 10, (▲) 15, (●) 20 min incubation time.

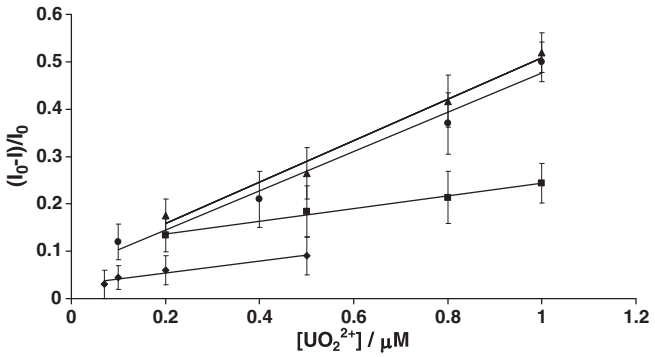

Fig. 2. Comparison of calibration curves towards uranyl acetate for ssDNA-modified electrode after 5 min incubation time: (■) 5-base probe sequence (5′-SH-$(CH_2)_6$-CGAC TG-3′); (▲) 10-base probe sequence (5′-SH-$(CH_2)_6$-CGACTGGTGAA-3′), (♦) 15-base probe sequence (5′-SH-$(CH_2)_6$-CGACTGGTGAATTCGT-3′); (●) 20-base probe sequence (5′-SH-$(CH_2)_6$-CGACTGTGAATTCGTAGCAG-3′).

important when methylene blue is used as a redox marker, as it shows a tendency to adsorb onto gold electrode surfaces [49]. In order to investigate the influence of electrode passivation on the biosensor response parameters, mixed monolayer was prepared. After oligonucleotide immobilization, the MCH solution was applied onto electrode surface. It is expected that MCH bounds to the electrode regions that are not occupied by oligonucleotide strands. Its application can also facilitate desorption of weakly adsorbed DNA strands. Calibration curves for 15 and 20-base probes were prepared for 5 (Fig. 3) and 60 min (data not shown) of incubation time.

As shown in Fig. 3a, the UO_2^{2+} calibration curve for electrode modified with 15-base ssDNA/MCH mixed monolayer shows relatively low slope (24.56 μM^{-1}) with good linear correlation ($R^2 = 0.9985$). The calibration slope for a sensor without MCH passivation was significantly higher (40.17 μM^{-1}), with slightly worse linear correlation

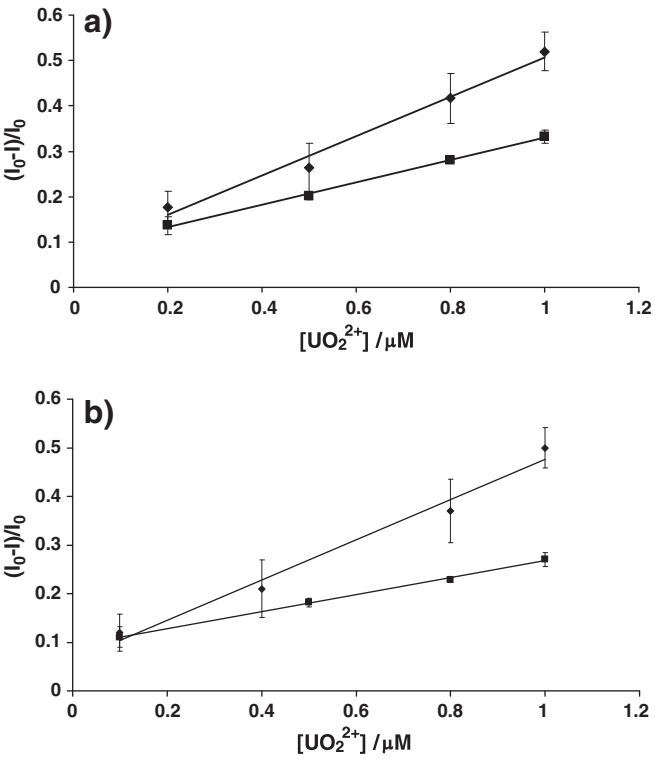

Fig. 3. Influence of additional electrode passivation on biosensor's response. a) electrode modified with 15-base probe ssDNA b) electrode modified with 20-base probe ssDNA. (■) without MCH; (▲) with MCH. Electrodes were incubated in uranyl acetate solution for 5 min.

($R^2 = 0.9774$). Analogous parameters were recorded for electrodes with receptor layers formed of 20-base probe oligonucleotides (Fig. 3b). The UO_2^{2+} calibration slopes were 17.5 μM^{-1} ($R^2 = 0.9981$) and 41.17 μM^{-1} ($R^2 = 0.9801$) for sensors with and without MCH, respectively. Results obtained for identical sensors, with 60 min sample incubation time, followed the same pattern. It can be concluded that mixed receptor monolayer (with MCH) decreases UO_2^{2+} calibration slopes, with concomitant improvement of linear correlation, as compared to oligonucleotide-only monolayers. Such behavior can be explained by the fact that MCH applied onto the oligonucleotide-modified electrode can replace some of the ssDNA probes, which leads to lower number of phosphate binding sites in the receptor layer. As a result, low slopes of the UO_2^{2+} calibration curves were observed. MCH presence also provides more repeatable quality of the DNA monolayer, as it eliminates weakly adsorbed oligonucleotides. This results in good linear correlation of the UO_2^{2+} calibration curves registered for electrodes modified with DNA/MCH mixed monolayers.

3.4. The influence of electrode area

Arguably, the biggest obstacle for the acceptance of biosensors as standard tools for industrial and clinical analysis is the requirement for pre-calibration [50]. It is theoretically possible to develop an electrochemical sensor, which does not require calibration, as the current passing through an electrochemical cell is proportional to the concentration of an electroactive analyte in the sample solution. Based on that, only one of the sensors from the whole production batch can be calibrated and the same calibration curve can be used for all other sensors. However, this is true only if all the measurement conditions, including electrode surface area, are constant. Obviously, electrode surface area can vary greatly, especially for mass-fabricated screen printed transducers, typically used for commercial electrochemical (bio)sensors. In the case of proposed UO_2^{2+}-selective biosensor, the signal is of differential nature, calculated as a difference of MB redox current measured before and after the incubation of the ssDNA-modified electrode in the sample solution containing uranyl ion. Thus, the electrode area might not be crucial for the biosensor response.

The influence of electrode surface on the magnitude of sensor response towards UO_2^{2+} cation (Table 2) was investigated with the use of gold disk electrodes that differ in geometrical surface area (electrode **1** −3.14 mm^2; electrode **2** −12.56 mm^2). Experiments were conducted for electrodes modified with 20-base ssDNA homogenous monolayer, as well as for electrodes modified with ssDNA/MCH mixed monolayer.

As shown in Table 2, the analytical signal (MB redox current change) is similar for electrodes with significantly different surface area, modified with DNA oligonucleotide receptor layer. In fact, current change is different by 10.5% for electrodes of 3.14 mm^2 and 12.56 mm^2 area. The use of the mixed monolayer (Table 2) gave even better results. In the case of the electrode of 3.14 mm^2 surface area, the current response is 0.7% higher than for a 12.56 mm^2 electrode. It can be concluded that in the proposed method, the change of working electrode area does not induce a meaningful difference in a biosensor response. Therefore, the developed biosensors could be produced as devices that require the calibration of one biosensor from whole production batch only.

Table 2
The influence of electrode surface area on a biosensor analytical signal. Analysis was carried out for a 5 min incubation time in 0.2 μM uranyl acetate solution for electrodes modified with ssDNA monolayer or ssDNA/MCH mixed monolayer.

A[a]/mm^2	$(I_0–I)/I_0$[b] ssDNA monolayer	$(I_0–I)/I_0$ ssDNA/MCH monolayer
3.14	0.162 ± 0.009	0.130 ± 0.004
12.56	0.179 ± 0.004	0.129 ± 0.013

[a] Electrode geometric surface area.
[b] I_0 −the MB current before the subjection of the sensor to UO_2^{2+} solution; I −the MB current after the subjection of the sensor to UO_2^{2+} solution.

Table 3
The effect of UO_2^{2+} exposure/removal cycles on the biosensor response. The regenerations (20 CV cycles) were performed in ammonium acetate buffer solution (50 mM, pH 7.0) containing 50 mM NaCl and 1 mM EDTA. The biosensor was modified with a ssDNA/MCH receptor layer. Each measurement was repeated 4 times.

Measurement no.	$(I_0–I)/I_0$[a]
1	0.260 ± 0.005
2	0.163 ± 0.033
3	0.152 ± 0.031
4	0.143 ± 0.032

[a] I_0 —the MB current before the subjection of the sensor to UO_2^{2+} solution; I —the MB current after the subjection of the sensor to UO_2^{2+} solution.

3.5. Sensor regeneration

In order to perform several determinations with the use of the same biosensor, the regeneration of DNA receptor layer is required. Accordingly, attempts were undertaken to remove uranyl cation from the receptor layer after sensor usage. Ammonium acetate solution (50 mM, pH 7.0), containing 50 mM NaCl and 1 mM EDTA as complexing agent, was used for this purpose. The regeneration procedure was as follows: after the first use for uranyl cation determination, the electrode was immersed in the regenerating solution and the set of 20 CV scans between −600 mV and 200 mV was performed. Subsequently, the electrode was washed with Tris–HCl solution and the procedure of UO_2^{2+} (1 μM) determination was repeated. The efficiency of the proposed regeneration method is shown in Table 3.

As it can be seen, the highest drop of the response signal (Δ change of 37.3%) occurred after first regeneration. However, the signal stabilizes during further re-exposure/removal cycles; unfortunately, the standard deviation of the results of these measurements is relatively high. It can be concluded that the DNA receptor layer can be regenerated with the use of EDTA-containing solution, although the regeneration procedure influences to some extent the analytical parameters of the biosensor.

4. Conclusions

In this work, several important modifications of the UO_2^{2+}-selective biosensor based on DNA oligonucleotides are described. Firstly, the efforts to improve UO_2^{2+} selectivity of ssDNA-based electrodes were undertaken. It was shown that by decreasing the amount of adenine nucleotides in the probe sequence, the interfering effect of Pb^{2+} ion can be greatly reduced. The influence of ssDNA probe length and incubation time on analytical parameters was also assessed. It was shown that for a 5 min incubation time, longer oligonucleotides (20 and 15 bases) induce higher sensitivity of UO_2^{2+} determination, as compared to shorter probes (10 and 5 bases). On the other hand, the increase of incubation time promotes the use of 10-base probe as it provides the highest sensitivity for incubation time of 60 min. The application of mixed monolayer, with MCH used for electrode passivation, improves the linear range of the biosensor response towards uranyl cation. However, the slope of the calibration curves decreases for sensors with such receptor layer. The electrochemical response of proposed sensor was found to be independent on the electrode surface area. To further improve the usefulness of proposed biosensor, the method for regeneration of the receptor layer was developed. Despite significant signal decrease after the first regeneration cycle, sensor response stabilizes during further re-exposure/removal cycles.

Acknowledgment

This work was financed by the Warsaw University of Technology and the Polish Ministry of Science and Higher Education within a framework of the Operational Programme —Innovative Economy, Priority I, Action 1.3, Sub-Action 1.3.1, project no. POIG.01.03.01-00-014/08-00.

References

[1] G.M. Whitesides, P.E. Laibinis, Wet chemical approaches to the characterization of organic surfaces: self-assembled monolayers, wetting, and the physical-organic chemistry of the solid–liquid interface, Langmuir 6 (1990) 87–96.
[2] I. Wenzl, C.M. Yam, D. Barriet, T.R. Lee, Structure and wettability of methoxy-terminated self-assembled monolayers on gold, Langmuir 19 (2003) 10217–10224.
[3] J.E. Houston, H.I. Kim, Adhesion, friction, and mechanical properties of functionalized alkanethiol self-assembled monolayers, Acc. Chem. Res. 35 (2002) 547–553.
[4] V.F. Petrenko, S. Peng, Reduction of ice adhesion to metal by using self-assembling monolayers (SAMs), Can. J. Physiol. 81 (2003) 387–393.
[5] T.D. Burleigh, Y. Gu, G. Donahey, M. Vida, D.H. Waldeck, Tarnish protection of silver using a hexadecanethiol self-assembled monolayer and descriptions of accelerated tarnish tests, Corrosion 57 (2001) 1066–1074.
[6] A.-R. El-Sayed, U. Harm, K.-M. Mangold, W. Fürbeth, Protection of galvanized steel from corrosion in NaCl solution by coverage with phytic acid SAM modified with some cations and thiols, Corros. Sci. 55 (2012) 339–350.
[7] J. Aizenberg, Patterned crystallisation on self-assembled monolayers with integrated regions of disorder, J. Chem. Soc. Dalton Trans. 21 (2000) 3963–3968.
[8] X. Wang, E. Ingall, B. Lai, A.G. Stack, Self-assembled monolayers as templates for heme crystallization, Cryst. Growth Des. 10 (2009) 798–805.
[9] C.-H. Shen, J.-C. Lin, Improving the surface biocompatibility with the use of mixed zwitterionic self-assembled monolayers prepared by a proper solvent, Langmuir 27 (2011) 7091–7098.
[10] A.S. Widge, M. Jeffries-El, X. Cui, C.F. Lagenaur, Y. Matsuoka, Self-assembled monolayers of polythiophene conductive polymers improve biocompatibility and electrical impedance of neural electrodes, Biosens. Bioelectron. 22 (2007) 1723–1732.
[11] J. Hu, J. Zhang, F. Liu, K. Kittredge, J.K. Whitesell, M.A. Fox, Competitive photochemical reactivity in a self-assembled monolayer on a colloidal gold cluster, J. Am. Chem. Soc. 123 (2001) 1464–1470.
[12] D.M. Adams, L. Brus, C.E.D. Chidsey, S. Creager, C. Creutz, C.R. Kagan, P.V. Kamat, X. Zhu, Charge transfer on the nanoscale: current status, J. Phys. Chem. B 107 (2003) 6668–6697.
[13] R. Naaman, Molecular controlled nano-devices, Phys. Chem. Chem. Phys. 13 (2011) 13153–13161.
[14] G.J. Leggett, Friction force microscopy of self-assembled monolayers: probing molecular organisation at the nanometre scale, Anal. Chim. Acta 479 (2003) 17–38.
[15] J.C. Love, L.A. Estroff, J.K. Kriebel, R.G. Nuzzo, G.M. Whitesides, Self-assembled monolayers of thiolates on metals as a form of nanotechnology, Chem. Rev. 105 (2005) 1103–1169.
[16] J.J. Gooding, N. Darwish, The rise of self-assembled monolayers for fabricating electrochemical biosensors-an interfacial perspective, Chem. Rec. 12 (2012) 92–105.
[17] J.H.T. Luong, K.B. Male, J.D. Glennon, Biosensor technology: technology push versus market pull, Biotechnol. Adv. 26 (2008) 492–500.
[18] D.K. Schwartz, Mechanisms and kinetics of self-assembled monolayer formation, Annu. Rev. Phys. Chem. 52 (2001) 107–137.
[19] J.J. Gooding, S. Ciampi, The molecular level modification of surfaces: from self-assembled monolayers to complex molecular assemblies, Chem. Soc. Rev. 40 (2011) 2704–2718.
[20] J. Labuda, A.M. Oliveira Brett, G. Evtugyn, M. Fojta, M. Mascini, M. Ozsoz, I. Palchetti, E. Paleček, J. Wang, Electrochemical nucleic acid-based biosensors: concepts, terms, and methodology (IUPAC Technical Report), Pure Appl. Chem. 82 (2010) 1161–1187.
[21] A.D. Ellington, J.W. Szostak, In vitro selection of RNA molecules that bind specific ligands, Nature 346 (1990) 818–822.
[22] T. Hianik, J. Wang, Electrochemical aptasensors —recent achievements and perspectives, Electroanalysis 21 (2009) 1223–1235.
[23] E. Palecek, M. Bartosik, Electrochemistry of nucleic acids, Chem. Rev. 112 (2012) 3427–3481.
[24] E. Farjami, R. Campos, J.S. Nielsen, K.V. Gothelf, J. Kjems, E.E. Ferapontova, Anal. Chem. 85 (2013) 121–128.
[25] S.C.B. Oliveira, O. Corduneanu, A.M. Oliveira-Brett, In situ evaluation of heavy metal-DNA interactions using an electrochemical DNA biosensor, Bioelectrochem 72 (2008) 53–58.
[26] E.E. Ferapontova, Electrochemical Indicators for DNA electroanalysis, Curr. Anal. Chem. 7 (2011) 51–62.
[27] Y. Shao, J. Wang, H. Wu, J. Liu, I.A. Aksay, Y. Lin, Graphene based electrochemical sensors and biosensors: a review, Electroanalysis 22 (2010) 1027–1036.
[28] C.B. Jacobs, M.J. Peairs, B.J. Venton, Review: carbon nanotube based electrochemical sensors for biomolecules, Anal. Chim. Acta 662 (2010) 105–127.
[29] E.L.S. Wong, E. Chow, J.J. Gooding, The electrochemical detection of cadmium using surface-immobilized DNA, Electrochem. Commun. 9 (2007) 845–849.
[30] P. Miao, L. Liu, Y. Li, G. Li, A novel electrochemical method to detect mercury(II) ions, Electrochem. Commun. 11 (2009) 1904–1907.
[31] Y. Lai, Y. Ma, L. Sun, J. Jia, J. Weng, N. Hu, W. Yang, Q. Zhang, A highly selective electrochemical biosensor for Hg^{2+} using hemin as a redox indicator, Electrochim. Acta 56 (2011) 3153–3158.
[32] D. Wu, Q. Zhang, X. Chu, H. Wang, G. Shen, R. Yu, Ultrasensitive electrochemical sensor for mercury(II) based on target-induced structure-switching DNA, Biosens. Bioelectron. 25 (2010) 1025–1031.
[33] X. Zhou, Q. Su, D. Xing, An electrochemiluminescent assay for high sensitive detection of mercury(II) based on isothermal rolling circular amplification, Anal. Chim. Acta 713 (2012) 45–49.
[34] X. Liu, C. Sun, H. Wu, Y. Zhang, J. Jiang, G. Shen, R. Yu, Label-free electrochemical biosensor of mercury ions based on DNA strand displacement by thymine-Hg(II)-thymine complex, Electroanal 22 (2010) 2110–2116.

[35] X. Yang, J. Xu, X. Tang, H. Liu, D. Tian, A novel electrochemical DNAzyme sensor for the amplified detection of Pb^{2+} ions, Chem. Commun. 46 (2010) 3107–3109.
[36] H. Zhang, B. Jiang, Y. Xiang, J. Su, Y. Chai, R. Yuan, DNAzyme-based highly sensitive electronic detection of lead via quantum dot-assembled amplification labels, Biosens. Bioelectron. 28 (2011) 135–138.
[37] Z. Lin, X. Li, H.B. Kraatz, Impedimetric immobilized DNA-based sensor for simultaneous detection of Pb^{2+}, Ag^{+}, and Hg^{2+}, Anal. Chem. 83 (2011) 6896–6901.
[38] X. Liu, W. Li, Q. Shen, Z. Nie, M. Guo, Y. Han, W. Liu, S. Yao, The Ag^{+}-G interaction inhibits the electrocatalytic oxidation of guanine —A novel mechanism for Ag^{+} detection, Talanta 85 (2011) 1603–1608.
[39] H. Gong, X. Li, Y-type, C-rich DNA probe for electrochemical detection of silver ion and cysteine, Analyst 136 (2011) 2242–2246.
[40] R. Ziółkowski, Ł. Górski, S. Oszwałdowski, E. Malinowska, Electrochemical uranyl biosensor with DNA oligonucleotides as receptor layer, Anal. Bioanal. Chem. 402 (2012) 2259–2266.
[41] A. Becker, H. Tobias, D. Mandler, Electrochemical determination of uranyl ions using a self-assembled monolayer, Anal. Chem. 81 (2009) 8627–8631.
[42] R. Banerjeea, Y. Katsenovichb, L. Lagosb, M. Sennc, M. Najad, V. Balsamoe, K.H. Pannellc, Ch. Li, Functional magnetic nanoshells integrated nanosensor for trace analysis of environmental uranium contamination, Electrochim. Acta 55 (2010) 7897–7902.
[43] R.K. Shervedani, S.A. Mozaffari, Preparation and electrochemical characterization of a new nanosensor based on self-assembled monolayer of cysteamine functionalized with phosphate groups, Surf. Coat. 198 (2005) 123–128.
[44] A. Tani, A.J. Thomson, J.N. Butt, Methylene blue as an electrochemical discriminator of single-and double-stranded oligonucleotides immobilised on gold substrates, Analyst 126 (2001) 1756–1759.
[45] M. Ortiz, A. Fragoso, P.J. Ortiz, C.K. O'Sullivan, Elucidation of the mechanism of single-stranded DNA interaction with methylene blue: a spectroscopic approach, J. Photochem. Photobiol. A Chem 218 (2011) 26–32.
[46] United States Environmental Protection Agency, http://www.epa.gov(Accessed 26 Oct 2012).
[47] R. Ziółkowski, Ł. Górski, M. Zaborowski, E. Malinowska, Application of mass fabricated silicon-based gold transducers for amperometric biosensors, Bioelectrochem 80 (2010) 31–37.
[48] J.M. Cooper, Biosensors, Oxford University Press, A practical approach, 2003.
[49] Y. Song, L. Wang, Well-ordered structure of methylene blue monolayers on Au(111) surface: electrochemical scanning tunneling microscopy studies, Microsc. Res. Tech. 72 (2009) 79–84.
[50] C. Creanga, S. Serban, R.W. Pittson, N.E. Murr, "No calibration" type sensor in routine amperometric bio-sensing: an example of a disposable hydrogen peroxide biosensor, in: P. Andrea (Ed.), Biosensors —Emerging Materials and Applications, InTech Rijeka, Croatia, 2011, pp. 141–152.